Optimal FOPID control for improved load frequency regulation of a renewable-integrated hybrid power system using the Puma optimizer

Mitali Samal[1], Chinmoy Kumar Panigrahi[1], Deepak Kumar Gupta[2]
[1]School of Electrical Engineering, KIIT Deemed to be University, Odisha, India
[2]Department of Electrical Engineering, Netaji Subhas University of Technology, New Delhi, India

Article Info

Article history:

Received Jan 14, 2026
Revised Jul 23, 2026
Accepted Aug 14, 2026

Keywords:

Fractional-order proportional-integral-derivative
Hybrid power system
Load frequency control
Particle swarm optimization
Puma optimizer

ABSTRACT

This study addresses the challenge of frequency stabilization in a complex two-area hybrid power system subjected to load disturbances. Area 1 comprises thermal, hydro, and wind power generation, while Area 2 integrates thermal, hydro, and gas turbine units, presenting a diverse and realistic system for control strategies. The inherent nonlinearities and varying dynamics of these generation sources, particularly wind power, necessitate a robust and advanced control solution. The proposed Puma optimizer-driven fractional-order proportional-integral-derivative (FOPID) controller is developed to enhance dynamic performance under load disturbances and renewable energy fluctuations. The proposed Puma optimizer-based fractional-order proportional–integral–derivative (PO-FOPID) controller is rigorously validated against a Puma optimizer-based proportional-integral-derivative (PO-PID) controller, a PSO-tuned PID controller, and a PSO-tuned fractional-order PID (PSO-FOPID) controller. The settling time and peak overshoot/undershoot are considered for comparison, while the integral of time multiplied by the absolute error (ITAE) performance index is used as the objective function to be minimized. The findings highlight the potential of combining Puma optimizer with fractional-order control for reliable frequency regulation in modern hybrid power systems.

Corresponding Author:

Chinmoy Kumar Panigrahi
School of Electrical Engineering, KIIT Deemed to be University
Bhubaneswar, Odisha, India
Email: panigrahichinmoy@gmail.com

1. INTRODUCTION

The increasing integration of conventional and renewable energy sources into hybrid power systems has made load frequency control (LFC) more challenging because of variations in generation, load demand, renewable intermittency, and operating conditions. These factors can cause significant frequency deviations and compromise system stability, highlighting the need for advanced and robust control strategies [1]-[3]. Accordingly, optimization-based, intelligent, adaptive, and fractional-order controllers have been extensively investigated. Particle swarm optimization (PSO) has been used to optimize proportional–integral–derivative (PID) controller parameters in single-area systems [4], while adaptive artificial neural network (ANN)-based PID control combined with the Grasshopper optimization algorithm (GOA) has been explored for controller optimization and comparative performance evaluation [5]. Fractional-order controllers provide additional tuning flexibility and have demonstrated promising performance in complex power-system applications. A cascade fractional-order PID (CFOPID) controller combining fractional-order PI and PD controllers has been proposed fortwo-area systems [6]. Similarly, a hybrid fractional-order PDμN–IλT controller optimized using the African vulture optimization algorithm (AVOA) achieved improved performance compared with PIDN, FOPID, and FOTID controllers [7].

Robust and decentralized approaches have also been developed to address system uncertainties and disturbances. A decentralized robust-adaptive controller incorporating a disturbance observer and linear matrix inequality (LMI)-based design, with genetic algorithm optimization, demonstrated robustness against load and renewable fluctuations without requiring inter-area information [8]. An integral derivative-tilted (ID-T) controller optimized using the Archimedes optimization algorithm (AOA) has also been investigated for multi-area, multi-source systems [9], while adaptive controllers have been applied to compensate for disturbances caused by intermittent photovoltaic (PV) and wave energy conversion systems (WECS) [10]. Intelligent, predictive, and optimization-based controllers have significantly enhanced LFC performance. Comparative studies of PID, fuzzy-PID, and MPC have demonstrated reduced frequency deviations in interconnected systems [11], while QCGO-optimized TD-TI control has shown robustness against renewable penetration, communication delays, load variations, and EV integration [12]. Event-triggered control further improves frequency regulation while reducing control effort [13]. FRT-PID with Dish-Stirling solar thermal systems and CHIOA optimization has achieved improved LFC performance [14]. MPCFC with ANN coordination has addressed demand-side resources and communication delays [15]. AO-FOPID, ISSA, BOA, and MHABC-PSO have further improved controller optimization [16]-[20]. LOA, AVOA, SCSO, IWO, OOA, and sampled-data approaches have addressed parameter tuning, delays, and sampling effects [21]-[23]. Cascaded FOPID, GWO-fuzzy PID, wind-power-prediction MPC, and Sinh Cosh-based controllers have demonstrated robust frequency regulation [24]-[27].

Hybrid optimization techniques have significantly improved controller tuning and load frequency control (LFC) performance. GA-PSO combines the global search capability of genetic algorithms with the rapid convergence of PSO to minimize ISE, IAE, ITAE, and ITSE indices [28]. HSCOA and improved ant colony optimization have enhanced PID and fuzzy-PID control under varying load conditions [29], [30]. Chaotic CSSO-GSA has improved settling time and ITAE, while GWO has demonstrated superior performance compared with genetic algorithms in multi-source systems [31], [32]. Notably, the Puma Optimizer (PO) provides effective exploration and exploitation capabilities, making it promising for optimal controller parameter tuning [33], [34]. Recent studies have further investigated Fuzzy-3D PID, FOIPDF, SMES-assisted fractional-order control, and intelligent controllers for renewable-integrated systems [35], [36]. Recent research increasingly incorporates renewable energy, electric vehicles (EVs), energy storage systems, and artificial intelligence. Reviews have highlighted classical, AI-based, MPC, sliding-mode, and cascade controllers for wind-integrated systems while identifying research gaps [37]. Fractional-order controllers optimized using QORSA, MOA, and related algorithms have demonstrated improved performance in renewable-integrated multi-area systems [38], [39]. Self-organized control using Selfish Herd Optimization has coordinated distributed energy resources (DERs), energy storage systems, and EVs through local frequency measurements [40]. Reinforcement-learning-based methods, including GSKO-assisted adaptive frequency control, DDPG-based supplementary control, and deep neural networks, have further enhanced LFC under renewable intermittency [41]-[43]. Finally, Black-winged Kite optimization and TID-MRAC approaches, supported by EV integration, have demonstrated improved resilience and frequency stability in renewable-rich microgrids and power systems [44], [45].

2. LEVERAGING ELECTRIC VEHICLES AND ENERGY STORAGE FOR GRID FREQUENCY REGULATION

Modern hybrid power systems increasingly integrate renewable energy sources, electric vehicles (EVs), and battery energy storage systems (BESS) to enhance grid flexibility and sustainability. The proposed PO-based FOPID controller can effectively coordinate these fast-response resources with conventional generating units to improve system damping, reduce settling time, and enhance frequency stability. The balanced power can be expressed as (1).

$$\Delta P_{bal} = \Delta P_{gen} + \Delta P_{EV} + \Delta P_{BESS} - \Delta P_{load} - \Delta P_{RES} \quad (1)$$

Where ΔP_{EV} → EV support power, ΔP_{BESS} → battery storage contribution, and ΔP_{RES} → renewable fluctuation power.

2.1. Two-area test system

This study employs a comprehensive two-area hybrid power system model to evaluate the performance of the proposed LFC strategy. The system is developed to reflect the complexity and challenges of modern power grids, which integrate conventional and renewable energy sources with vastly different dynamics. As illustrated in the schematic diagram (Figure 1), the system comprises two interconnected control areas, each with a distinct generation portfolio to reflect a realistic and challenging scenario for frequency regulation. Area 1 is configured with a thermal power plant, a hydro power plant, and a wind power plant. Area 2 comprises a thermal power plant, a hydro power plant, and a gas turbine unit. This portfolio represents conventional generation technologies with contrasting response times. The gas turbine, in particular, provides essential fast-ramping capability to balance system fluctuations.

A step load perturbation (SLP) is applied in Area 1 to simulate a sudden change in power demand, representing a standard yet critical disturbance for testing the dynamic performance of the LFC system. The primary objective of the LFC mechanism in this test system is to maintain system frequency in both areas and regulate the tie-line power flow to its scheduled value following a load disturbance. The diverse nature of the generation sources, each with unique transfer functions, time constants, governor-turbine dynamics, and nonlinearities (such as generation rate constraints (GRC) and Governor dead band (GDB)), creates a highly complex and high-order system model. This complexity establishes a rigorous test system for assessing the robustness, adaptability, and superiority of advanced control techniques over conventional methods.

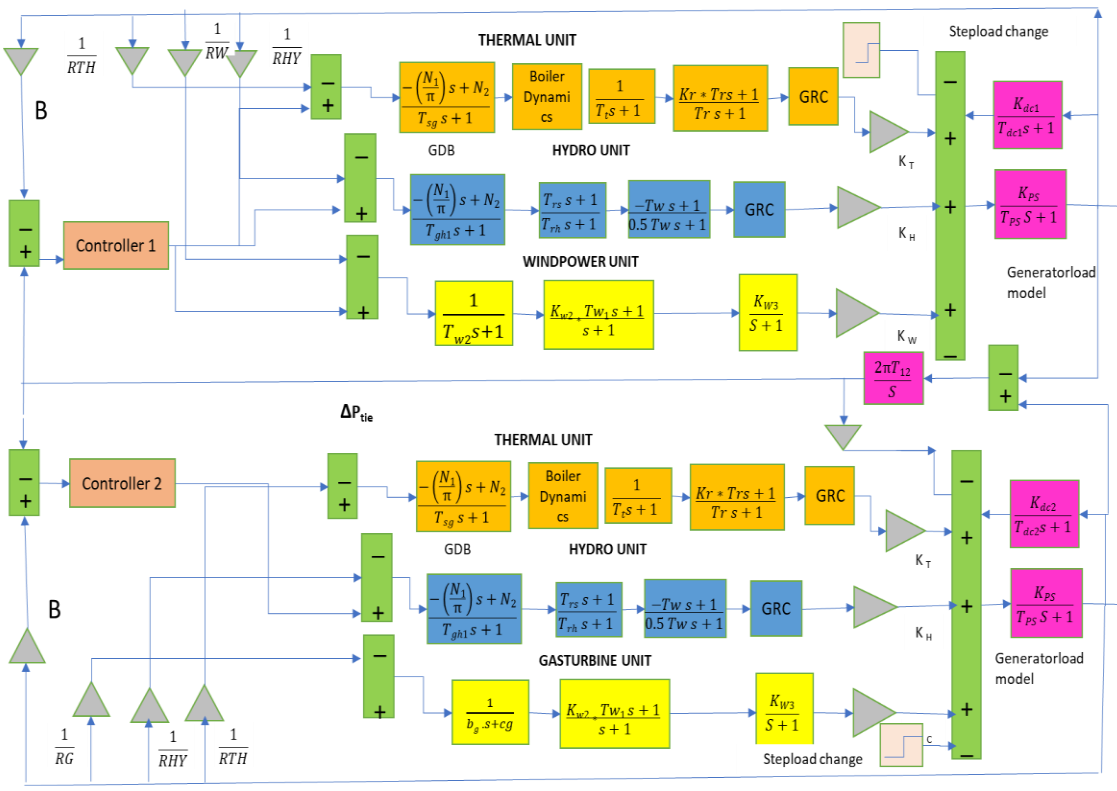

Figure 1. Transfer function block diagram of a two-area hybrid power system

3. MATHEMATICAL MODELLING OF SYSTEM COMPONENTS

This section presents the mathematical models of the major components in the hybrid power system. The dynamic behavior of each subsystem is formulated using transfer functions to facilitate load frequency control analysis and controller design. where Figure 2(a) represents the boiler dynamics associated with a conventional thermal generating unit. Figure 2(b) represents the generation rate constraint (GRC) of a thermal generating unit. Figure 3 represents the generation rate constraint of a hydro generating unit.

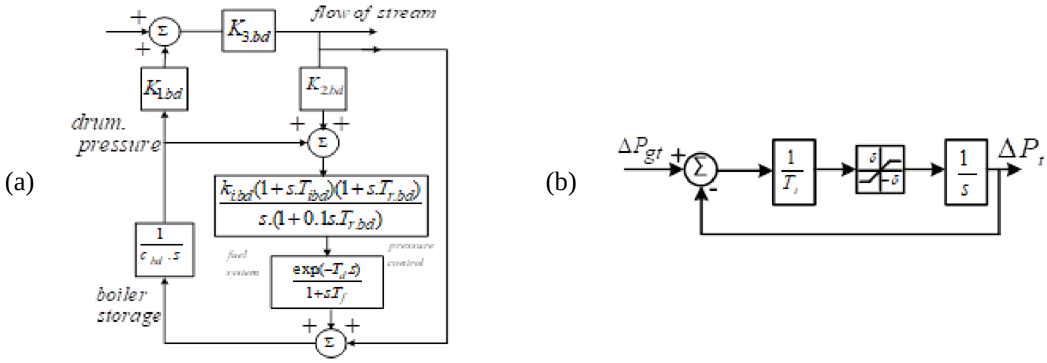

Figure 2. Block diagram of thermal unit: (a) boiler dynamics and (b) GRC

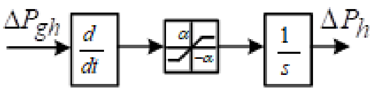

Figure 3. GRC in hydro unit

4. FRACTIONAL ORDER PID CONTROLLER

Figure 4 depicts the architecture of the proposed FOPID controller. Within this framework, the integral and derivative terms are generalized into fractional orders, represented by λ and μ, respectively. The corresponding mathematical formulation of the controller is expressed as (2).

$$C(s) = u(s)/e(s) = K_p + K_i/s^{\lambda} + K_d s^{\mu} \quad (2)$$

Where K_p, K_i, and K_d are the proportional, integral, and derivative gains; λ is the order of integration; μ is the order of differentiation; e(t) is the input error; and u(t) is the output of the controller. By fine-tuning the fractional orders, the FOPID controller can effectively reduce overshoot, improve settling time, and minimize integral error indices such as ITAE.

$$ITAE = \int_0^{t_{sim}} t * |e(t)| dt \quad (3)$$

Where t_{sim} is the simulation time. In the current research work, parameters of FOPID controllers have been fine-tuned with the Puma optimizer (PO) algorithm by minimizing the ITAE objective function.

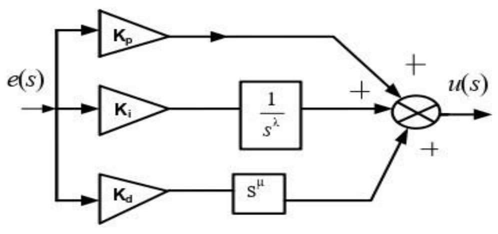

Figure 4. Block diagram of the FOPID controller

5. IMPACT OF COMMUNICATION DELAY ON LFC PERFORMANCE

The proposed PO-FOPID controller provides improved robustness against communication latency due to the enhanced flexibility offered by fractional-order dynamics and the efficient tuning capability of the Puma Optimizer algorithm. The communication delay $e^{-s\tau d}$, which is expressed by Taylor series expansion as (4).

$$e^{-s\tau d} = \frac{1-\frac{Td}{2}s}{1+\frac{Td}{2}s} \quad (4)$$

The communication delay transfer function in a load frequency control (LFC) system is expressed as (5).

$$Gd(s) = e^{-s\tau} \quad (5)$$

The transfer-function block diagram of a two-area hybrid power system considering communication time delays (CTDs) in Figure 5 represents the dynamic relationship between generation, load demand, and frequency. Each area includes governor, turbine, and power-system models, interconnected through tie-line power. CTDs are represented by e^{-sTd}, capturing communication delays and their effects on frequency stability and LFC performance.

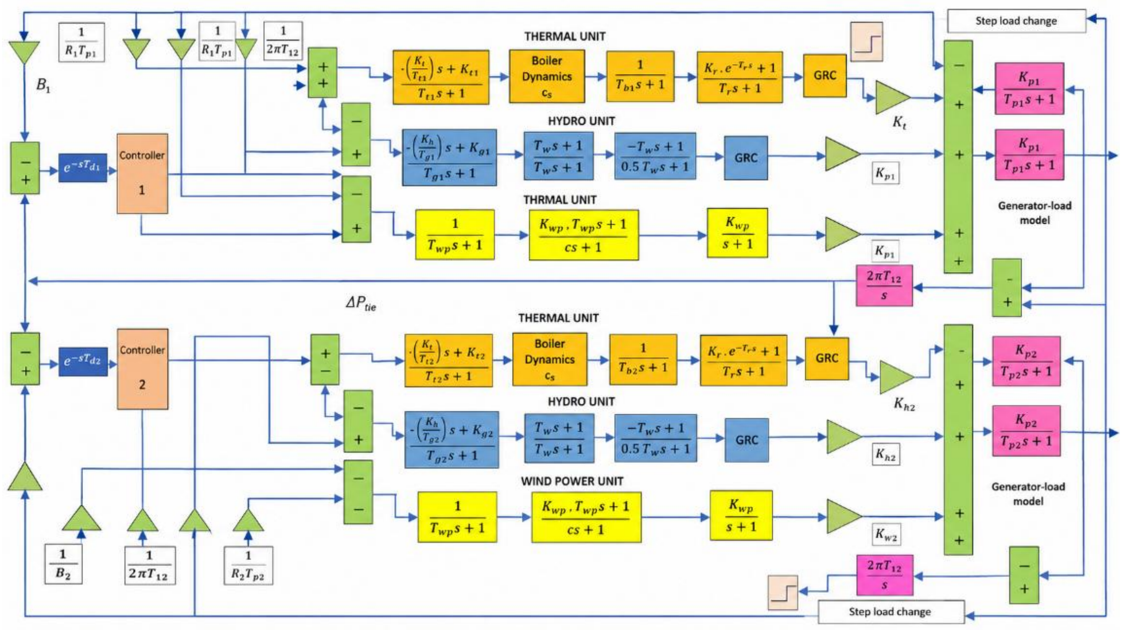

Figure 5. Transfer function block diagram of a two-area hybrid power system considering CTDs

6. PUMA OPTIMIZER (PO) ALGORITHM

The Puma optimizer (PO) is a recently developed metaheuristic algorithm inspired by the social dynamics and hunting strategies of Pumas [22]. The most optimal solution within the population is designated as the male Puma, which represents the best-known position in the search space. The remainder of the population, comprising other candidate solutions, is modeled as female Pumas distributed throughout the territory, which corresponds to the entire optimization landscape. A distinctive feature of the PO algorithm is its dynamic phase-switching mechanism. At each iteration, every solution candidate autonomously selects between two fundamental phases: exploration and exploitation. This adaptive strategy allows the algorithm to effectively balance global search intensification with local search refinement. The flowchart of the Puma Optimizer is shown in Figure 6.

6.1. Exploration phase: territorial roaming

The exploration phase in PO is modeled after the natural behavior of Pumas traversing their territory over long distances to locate prey. This process involves investigating diverse regions, including both previously fruitful areas and unexplored sections of the territory. Mathematically, this translates to large-scale movements within the search space, enabling the algorithm to escape local optima and discover promising new regions. The movement during this phase is guided by a combination of the global best solution (the male Puma's position) and stochastic factors, ensuring a robust and widespread search.

6.2. Exploitation phase: prey capture strategies

Once a promising area is identified, the algorithm switches to the exploitation phase, which employs two distinct operators inspired by the Puma's primary hunting techniques: ambushing and running. These operators facilitate intensive local search around promising solutions. The ambush strategy simulates the Puma's patient, stealthy approach, involving subtle and precise movements to refine the solution's position. The running strategy emulates a more direct and rapid pursuit, allowing for quicker convergence towards a local optimum. By leveraging these two tactics, the PO algorithm can effectively navigate the complex topography of the solution space, enhancing the quality of solutions through focused local search.

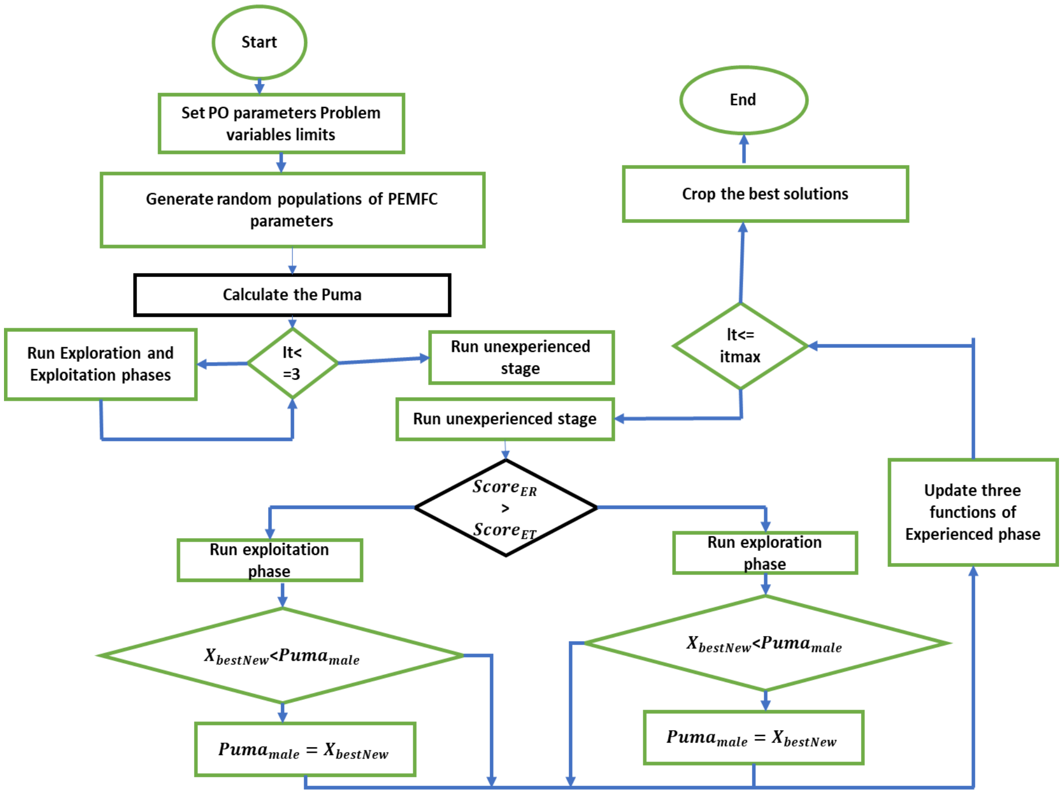

Figure 6. Flowchart of the PO optimization technique

6.3. Phase switching mechanism

The core of the PO's adaptability lies in its phase-switching criterion. This mechanism probabilistically determines whether an individual agent will engage in exploration or exploitation during an iteration. The decision is often based on control parameters that can be tuned, allowing the algorithm to prioritize broad exploration in the early stages and intensify exploitation as the search progresses. All these operations are expressed by (6) and (7).

$$f1_{exp\,loration} = PF_1 . \frac{Seq^1{}_{Cos\,tExplore}}{Seq_{Time}} \quad (6)$$

$$f1_{exp\,loitation} = PF_1 . \frac{Seq^1{}_{Cos\,tExploit}}{Seq_{Time}} \quad (7)$$

During the exploration phase, the cost of the best solution candidates is calculated as (8).

$$Seq^1{}_{Cos\,tExplore} = Cos\,t\,Initial_{Best} - Cost1_{Explore} \quad (8)$$

In (8), $Cost1Explore$ denotes the cost of the best solution achieved in the first iteration. After completing the third iteration, the Pumas are considered experienced and must decide between entering the exploration or exploitation phase. To make this decision, the scores are computed as in (9) and (10).

$$ScoreExploration = (PF1.f1_{Exploration}) + (PF2.f2_{exp\,loration}) \quad (9)$$

$$ScoreExploitation = (PF1.f1_{Exploitation}) + (PF2.f2_{exp\,loitation}) \quad (10)$$

According to (9) and (10) if '*ScoreExploration*' is greater than '*ScoreExploitation*' then the exploration phase is selected. Puma optimizer algorithm is used to optimally tune the parameters of the FOPID controller by minimizing the ITAE performance index given in (2).

Conventional PI and PID controllers are widely used in practical power systems due to their simple structure and ease of implementation; however, their performance significantly degrades under nonlinear operating conditions, renewable intermittency, and parameter uncertainties. Advanced controllers such as model predictive control (MPC), fuzzy logic controllers, and adaptive control techniques provide improved dynamic performance but often involve higher computational complexity, extensive rule-base design, or the requirement of accurate system models. Compared with these approaches, the proposed PO-FOPID controller combines the flexibility of fractional-order control with the efficient global optimization capability of the Puma optimizer, as shown in Table 1.

Table 1. Comparison between advanced controllers

Controller	Settling time	Overshoot	Robustness	Computational complexity
PI	High	High	Moderate	Low
PID	Moderate	Moderate	Moderate	Low
Fuzzy	Moderate	Low	Good	Moderate
Adaptive	Low	Low	Good	High
MPC	Very low	Very low	Excellent	Very high
PO-FOPID	Very low	Very low	Excellent	Moderate

7. RESULTS AND DISCUSSION

The proposed PO-FOPID controller is evaluated through MATLAB/Simulink simulations on a two-area hybrid power system comprising thermal, hydro, wind, and gas units. The controller is compared with PO-PID, PSO-PID, and PSO-FOPID approaches using performance indices including settling time, peak overshoot/undershoot, and ITAE.

7.1. Case study I (load variation)

A step load disturbance test was conducted to evaluate system performance, wherein Area 1's demand was subjected to a 1% increase while Area 2's load was held fixed. The resulting PID and FOPID controller gains, optimized via the PSO algorithm and Puma Optimizer (PO), are summarized in Table 2. The performance of these controllers was evaluated in terms of overshoot and settling time for the frequency deviations (Δf_1 and Δf_2) and tie-line power deviation (ΔP_{12}). The corresponding results are presented in Table 3, and the dynamic responses are illustrated in Figure 7.

Table 2. Controller parameters tuned with different optimization techniques

Controller parameters	PSO-based PID controller	PO-based PID controller	PSO-based FOPID controller	PO-based FOPID controller (proposed)
KP1	3.2553	3.207759423	0.1766	2.978045323
KI1	2.5541	4.245906343	6.0788	3.176984215
KD1	0.1	0.390933847	2.2741	0.405766887
λ1	***	***	0.751	0.962848639
μ1	***	***	0.6529	0.90987994
KP2	1.8529	3.646991103	0.9153	0.543676343
KI2	9.449	0.111202651	9.1071	10
KD2	1.5608	0.665154237	0.2553	0.483217698
λ2	***	***	0.5627	0.5
μ2	***	***	0.9608	0.5
ITAE	0.5038	0.28838	0.4562	0.23313

The proposed PO-FOPID controller demonstrated a clear improvement over the other methods. The settling times achieved were 5.4 s for Δf_1, 10.2 s for Δf_2, and 9.9 s for ΔP_{12}. These values are significantly lower compared to those obtained with PSO-PID (10.6 s, 25.3 s, 14.2 s), PO-PID (5.8 s, 15.2 s, 15.3 s), and PSO-FOPID (5.7 s, 10.6 s, 10.2 s). The results indicate that the PO-FOPID controller not only minimizes settling time but also maintains system stability more effectively.

The perturbed response of frequencies and tie-line power represents the dynamic behavior of a two-area hybrid power system following a load or generation disturbance. The frequency deviations, Δf_1 and Δf_2, indicate the stability of Areas 1 and 2, while the tie-line power deviation, ΔP_{tie}, represents the power exchange between the areas as shown in Figure 7. An effective controller should produce smaller peak deviations, faster settling time, reduced oscillations, and minimum steady-state error, demonstrating improved frequency regulation and inter-area power stability.

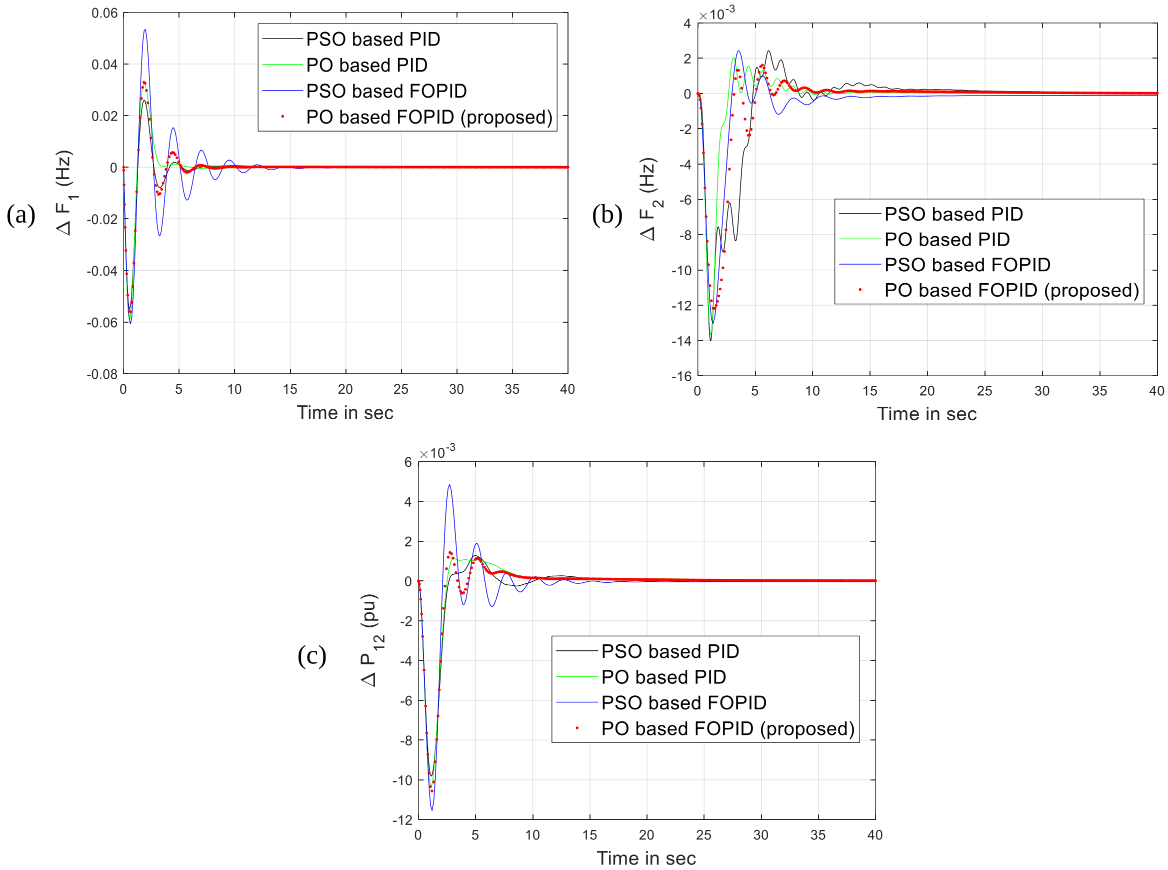

Figure 7. Perturbed response of frequencies and tie-line power Case I: (a) frequency response of Area-1 (b) frequency response of Area-2, and (c) response of tie-line power

A key observation is the superior damping capability of the proposed controller. The PO-FOPID design reduced oscillations quickly, preventing sustained deviations that can compromise stability in interconnected systems. Unlike the other controllers, it adapted smoothly to load disturbances without producing noticeable overshoot or extended transients. This balance between fast response and controlled damping is essential for hybrid power systems, where renewable energy sources add significant variability and uncertainty. Further, to evaluate robustness, λ and μ were independently perturbed around their optimized nominal values by ±10%, while maintaining all other controller gains unchanged. The effects on frequency deviations (Δf_1 and Δf_2), tie-line power deviation (ΔP_{12}), settling time, overshoot, and ITAE performance index were analyzed under step load disturbance conditions, and the comparison graphs are shown in Figure 8.

Based on the simulation results and waveform outputs, the proposed controller can be confirmed to preserve stability in the two-area system. A comparison of the optimization methods was also carried out with respect to their convergence behavior. As shown in Figure 9, the PO-based FOPID method exhibits noticeably better convergence performance relative to the other techniques.

To further verify the closed-loop stability of the proposed hybrid power system, a small-signal stability analysis was carried out using frequency-domain techniques illustrated in Figure 10. The Bode plot of the closed-loop hybrid power system with the Puma optimizer (PO)-tuned FOPID controller illustrates the system's frequency-domain stability and dynamic characteristics. The magnitude plot indicates the gain response, while the phase plot represents phase variation with frequency. The corresponding gain margin and phase margin are important indicators of robustness. A positive gain margin and phase margin confirm adequate stability, while a smooth magnitude response and sufficient bandwidth indicate effective frequency regulation and improved disturbance rejection. The Bode diagram of the closed-loop system with the proposed PO-FOPID controller indicates sufficient stability, with a gain margin of 16.3 dB and a phase margin of 73.4 degrees, ensuring stable operation under load disturbances and parameter uncertainties.

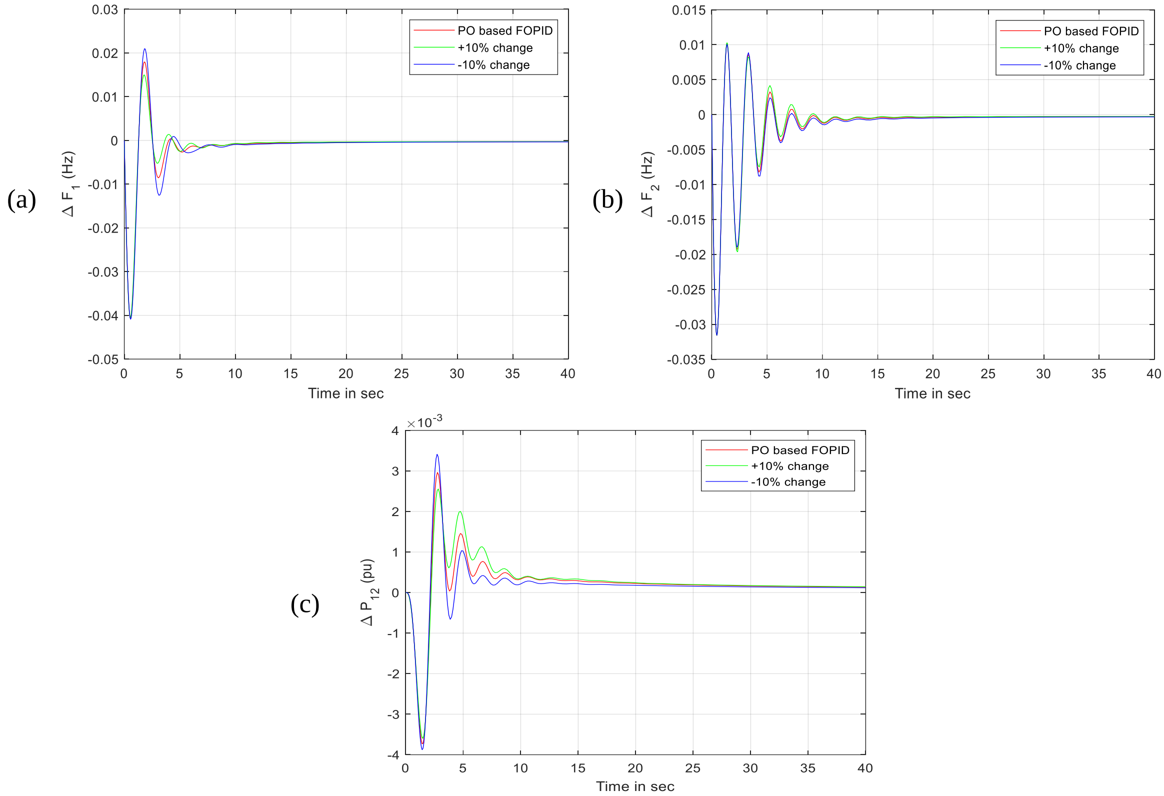

Figure 8. Perturbed response of frequencies and tie-line power- varying λ and μ: (a) frequency response of Area-1, (b) frequency response of Area-2, and (c) Response of tie-line power

Table 3. Settling time and overshoot

Case I			
System configuration	States	Overshoot (p.u.)	Settling time (sec)
PSO-based PID controller	ΔF_1	-0.054	10.6
	ΔF_2	-0.013	25.3
	ΔP_{12}	-0.009	14.2
PO-based PID controller	ΔF_1	-0.058	5.8
	ΔF_2	-0.0138	15.2
	ΔP_{12}	-0.0102	15.3
PSO-based FOPID controller	ΔF_1	-0.067	5.7
	ΔF_2	-0.0124	10.6
	ΔP_{12}	-0.0108	10.2
PO-based FOPID controller (proposed)	ΔF_1	-0.056	5.4
	ΔF_2	-0.012	10.2
	ΔP_{12}	-0.01	9.9
PO-based FOPID controller (proposed) (increasing μ by 10%)	ΔF_1	-0.067	6.1
	ΔF_2	-0.048	11.3
	ΔP_{12}	-0.032	10.3
PO and FOPID controller (proposed) (increasing λ and μ by 10%)	ΔF_1	-0.047	4.8
	ΔF_2	-0.096	9.7
	ΔP_{12}	-0.009	8.6

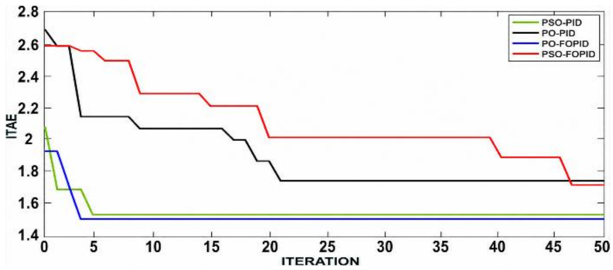

Figure 9. Convergence characteristics for PSO-FOPID, PSO-PID, PO-PID, and PO-FOPID

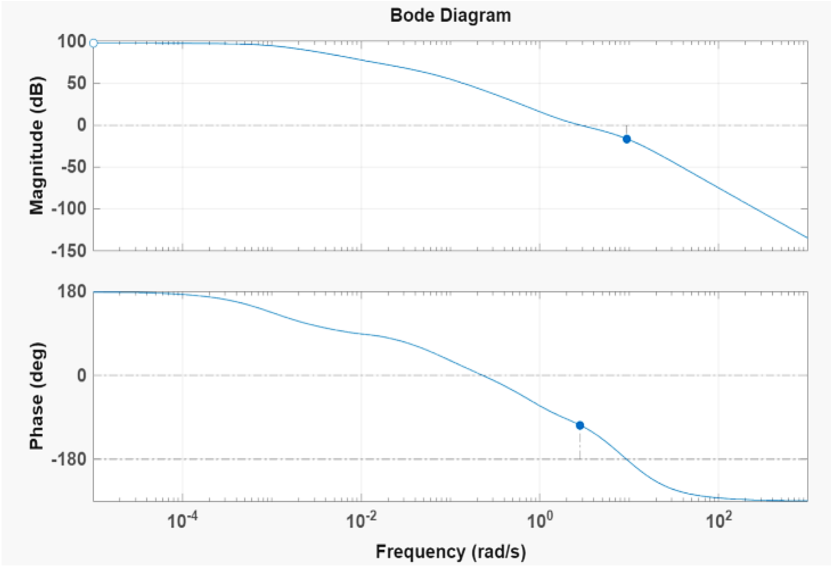

Figure 10. Bode plot of closed-loop hybrid power system with PO-FOPID controller

7.2. Case study II (load variation)

To evaluate the robustness of the system response to a step load disturbance, a 1% increase in demand in Area-1 and a 2% increase in load in Area-2 were applied. The PID and FOPID controller parameters were optimized using particle swarm optimization (PSO) and the Puma optimizer (PO), and the resulting tuned values are summarized in Table 4. Controller performance was assessed based on overshoot and settling time of the frequency deviations (Δf_1 and Δf_2) as well as the tie-line power deviation (ΔP_{12}). The numerical outcomes are reported in Table 5, and the corresponding time-domain responses are depicted in Figure 11.

The proposed controller demonstrates enhanced damping performance by rapidly suppressing oscillations and maintaining system stability with less overshoot and settling time, as shown in Table 5. Settling time and overshoot are key performance indices used to evaluate the dynamic response of the proposed PO-FOPID-controlled hybrid power system. Settling time **(**T_s**)**indicates how quickly the frequency and tie-line power responses return to their steady-state values, while overshoot **(**M_p**)** represents the maximum deviation beyond the desired response. Lower T_s and M_p indicate faster, smoother, and more stable frequency regulation. The PO-FOPID controller responds smoothly to load disturbances, avoiding excessive overshoot and long transients. The proposed controller is robust and performs well with CTDs.

Table 4. Controller parameters tuned with different optimization techniques

Controller parameter	PSO-based PID	PO-based PID	PSO-based FOPID	PO-based FOPID (proposed)
KP1	3.4306	3.221176	0.1384	2.8478
KI1	7.9298	3.964461	4.2506	3.2129
KD1	1.2102	0.417512	2.06	0.5996
λ1	***	***	0.7529	0.9529
µ1	***	***	0.7353	0.6627
KP2	3.2553	4.75636	2.7133	2.2714
KI2	8.4557	0.846819	4.6733	4.9231
KD2	0.5675	0.1	0.1	0.638
λ2	***	***	0.9216	0.8216
µ2	***	***	0.8608	0.9255
ITAE	0.4531	0.28715	0.2784	0.2568

7.3. Case study III (robustness check with varying step load)

The resilience of the proposed PO-based FOPID controller was examined under conditions of frequent load disturbances. To test adaptability, step load variations were introduced in the control areas at 15-second intervals. Figure 12 illustrates the corresponding frequency responses in Areas 1 and 2, along with tie-line power deviations subjected to varying load changes.

The robustness of the proposed PO-based FOPID controller is evaluated under consecutive step load disturbances applied every 15 s, assessing its adaptability, dynamic tracking capability, and resilience against continuous demand fluctuations in interconnected power systems. As shown in Figure 12, the load in Area-1 was varied in a stepwise manner at uniform time intervals, while the remaining area parameters were maintained unchanged. The resulting system responses, including frequency deviations in Areas 1 and 2 and the tie-line power deviation, are presented in Figure 13. The PO-FOPID controller effectively mitigates the impact of successive disturbances by rapidly damping oscillations and restoring system variables to their nominal values after each load change.

Table 5. Settling time and overshoot

Case II			
System configuration	States	Overshoot (p.u.)	Settling time (sec)
PSO-based PID controller	ΔF_1	-0.016	21.2
	ΔF_2	-0.008	15.3
	ΔP_{12}	-0.003	26.01
PO-based PID controller	ΔF_1	-0.008	24.1
	ΔF_2	-0.008	22.8
	ΔP_{12}	-0.003	24.60
PSO-based FOPID controller	ΔF_1	-0.009	16.5
	ΔF_2	-0.004	16.2
	ΔP_{12}	-0.002	31.6
PO-based FOPID controller (proposed)	ΔF_1	-0.009	13.4
	ΔF_2	-0.007	14.40
	ΔP_{12}	-0.003	11.60
PO-based FOPID controller (proposed) (with CTDs)	ΔF_1	-0.013	15.6
	ΔF_2	-0.011	16.30
	ΔP_{12}	-0.004	13.30

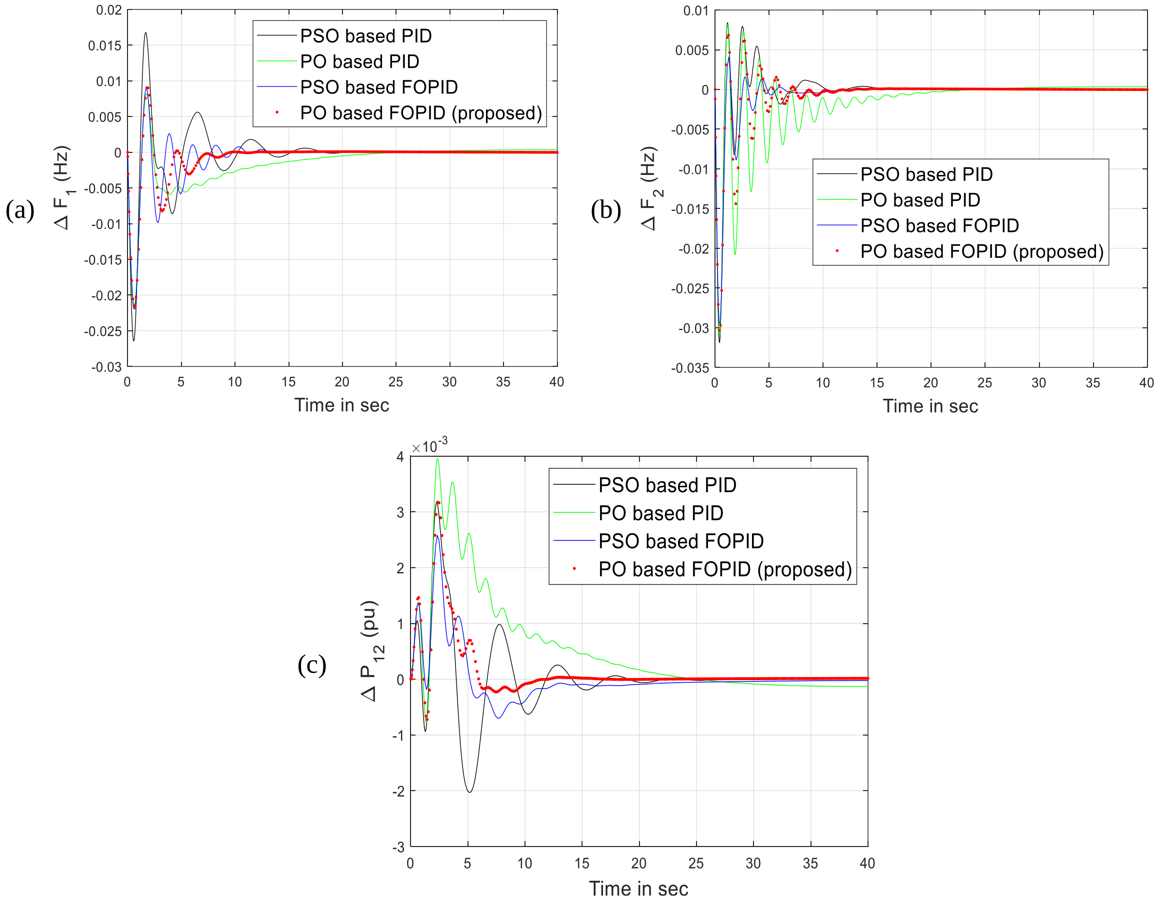

Figure 11. Perturbed response of frequencies and tie-line power: (a) frequency response of Area-1, (b) frequency response of Area-2, and (c) response of tie-line power

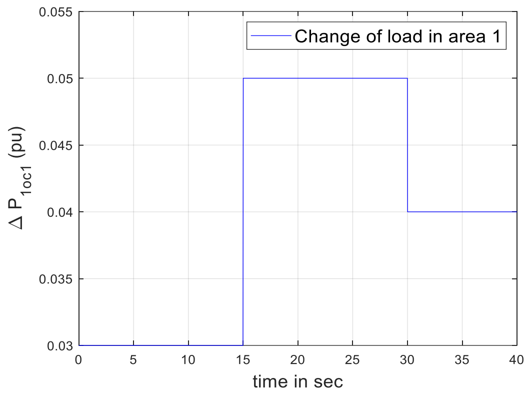

Figure 12. Step load variation in Area 1

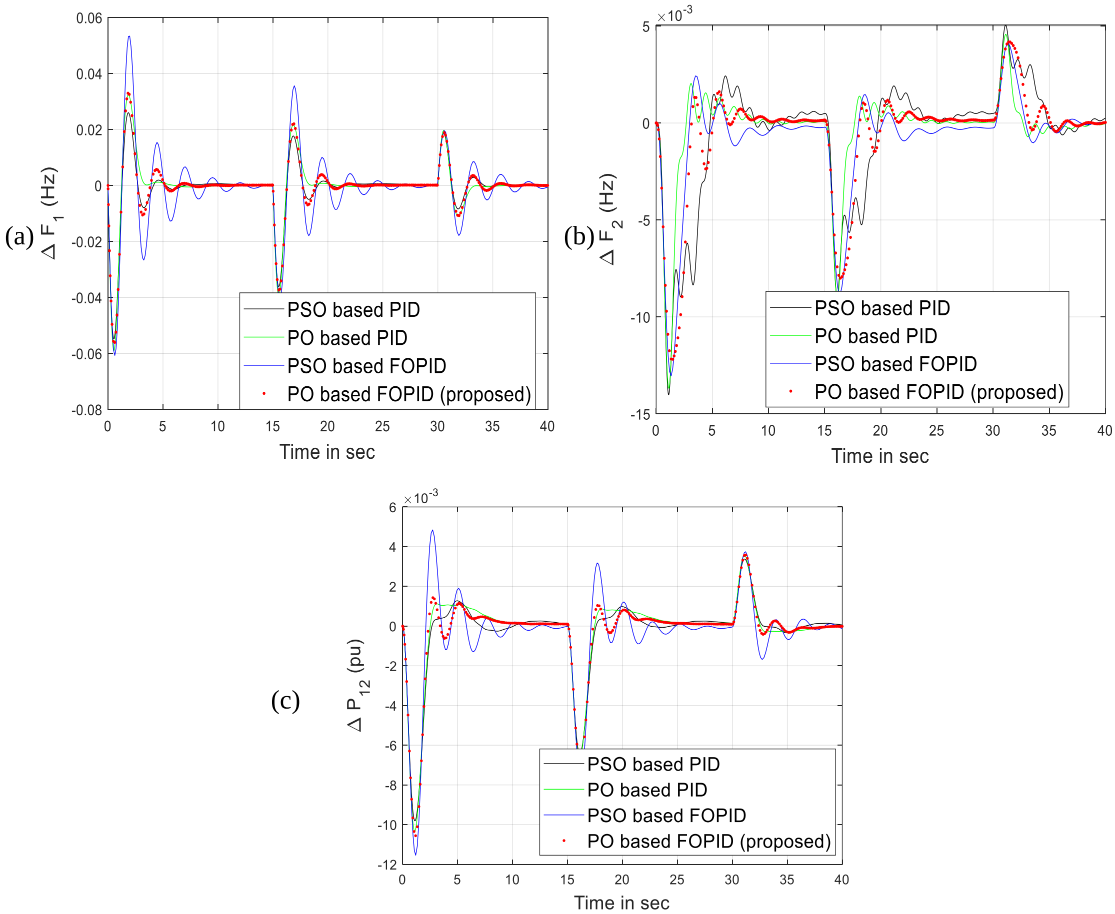

Figure 13. Perturbed response of frequencies and tie-line power for Case III: (a) frequency response of Area-1, (b) frequency response of Area-2, and (c) response of tie-line power

7.4. Case study IV: sensitivity analysis

To evaluate the resilience of the LFC controller across different dynamic conditions, a sensitivity study was carried out by systematically varying the turbine (Tt) and governor (Tg) time constants. Simulations performed under multiple system configurations validated the effectiveness of the proposed load frequency control (LFC) scheme. In particular, both Tt and Tgh were varied by ±25% to assess the controller's robustness and sensitivity. The resulting frequency deviations in Areas 1 and 2, along with the corresponding tie-line power fluctuations following a 25% variation in Tt and Tg, are presented in Figure 14.

The proposed PO-based FOPID controller demonstrates excellent robustness under successive load disturbances by providing faster stabilization, reduced oscillations, and improved frequency regulation. Its fractional-order structure enhances transient performance and resilience against nonlinearities, renewable intermittency, and communication delays. Furthermore, the decentralized ACE-based architecture enables straightforward scalability to multi-area interconnected power systems, with independent Puma Optimizer tuning ensuring effective frequency stabilization across diverse generation sources.

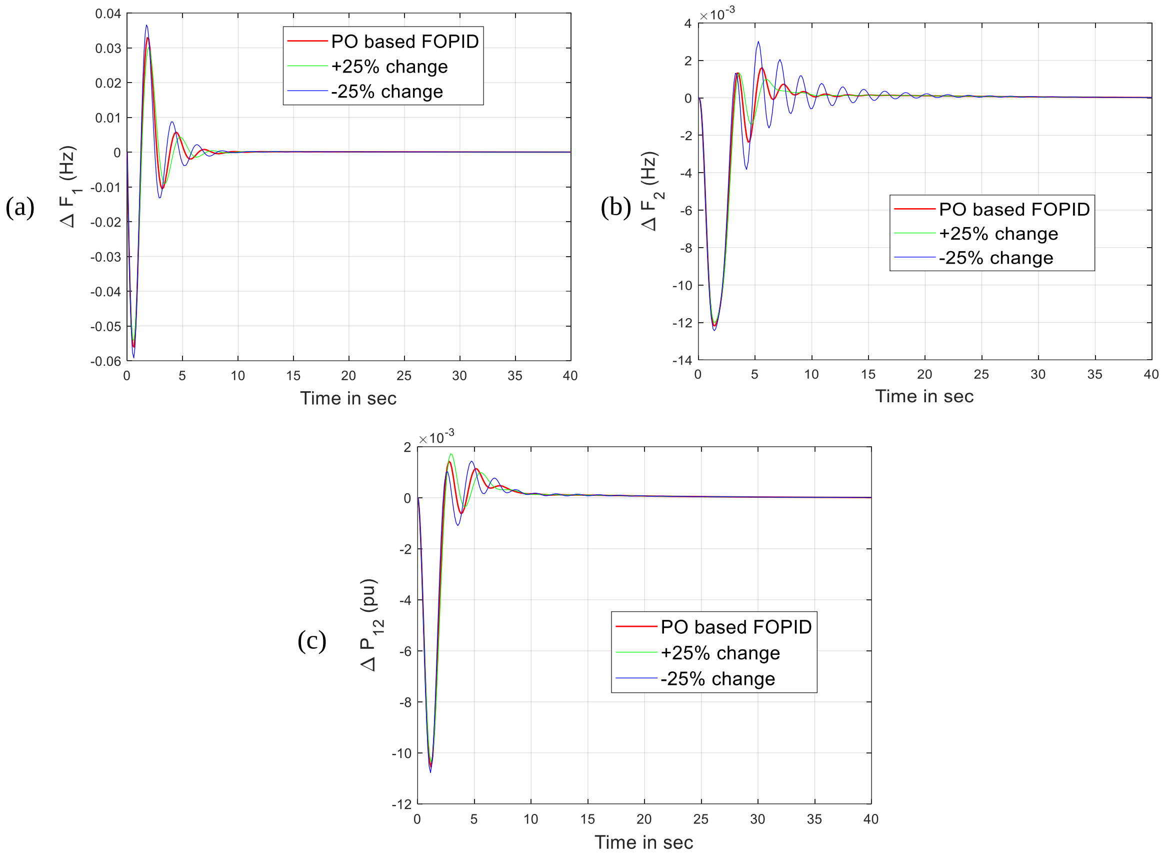

Figure 14. Perturbed response of frequencies and tie-line power for Case IV with altered Tt and Tg values: (a) frequency response of Area-1, (b) frequency response of Area-2, and (c) response of tie-line power

7.5. Computational complexity analysis

The computational complexity of the proposed Puma optimizer (PO) based FOPID controller was analyzed to evaluate its suitability for practical load frequency control applications. In population-based optimization algorithms, the computational burden mainly depends on the population size, number of iterations, dimensionality of the optimization problem, and objective function evaluation.

The comparison of PSO, GWO, WOA, GOA, and the proposed Puma Optimizer (PO) in terms of computational complexity, convergence speed, ability to avoid local minima, and real-time feasibility has been demonstrated in Table 6. PSO provides good real-time feasibility but has relatively weak local-minima avoidance and moderate convergence speed. GWO offers fast convergence with moderate local-minima avoidance, while WOA and GOA demonstrate moderate convergence and local-minima avoidance capabilities. In comparison, the proposed PO algorithm provides fast convergence and strong local-minima avoidance, thereby improving the probability of obtaining high-quality optimal solutions.

Table 6. Computational complexity comparison

Algorithm	Computational complexity	Convergence speed	Local minima avoidance	Real-time feasibility
PSO	(O (N\times Iter\times D))	Moderate	Weak	Good
GWO	(O (N\times Iter\times D))	Fast	Moderate	Good
WOA	(O(N\times Iter\times D))	Moderate	Moderate	Good
GOA	(O(N\times Iter\times D))	Moderate	Moderate	Good
PO (Proposed)	(O(N\times Iter\times D))	Fast	Strong	Excellent

8. CONCLUSION

The paper demonstrates that the Puma optimizer–based FOPID controller provides a more reliable solution for frequency regulation in a hybrid two-area power system. The combination of thermal, hydro, wind, and gas turbine units brings nonlinear and uncertain dynamics that challenge traditional control methods. The proposed controller addresses these issues by ensuring quicker settling, lower overshoot, and reduced error indices compared with PO-PID, PSO-PID, and PSO-FOPID alternatives. Settling time improvement: Under a 1% step load disturbance in Area-1, the proposed PO-FOPID controller achieved settling times of 5.4 s (Δf_1), 10.2 s (Δf_2), and 9.9 s (ΔP_{12}). The error index reduction (ITAE) value obtained using PO-FOPID was 0.23313, which is 53.7% lower than PSO-PID (0.5038),19.1% lower than PO-PID (0.28838), and 48.9% lower than PSO-FOPID (0.4562). For simultaneous load variations (1% in Area-1 and 2% in Area-2), the PO-FOPID controller reduced the settling time of tie-line power deviation to 11.6 s, compared to 26.01 s (PSO-PID) and 31.6 s (PSO-FOPID)—an improvement exceeding 55%. Even with ±25% variations in turbine and governor time constants, the proposed controller maintained stable frequency regulation with minimal deviation, confirming strong robustness against parameter uncertainties. These results suggest that integrating advanced optimization with fractional-order control can significantly improve stability in power systems with high renewable penetration, offering a practical pathway for future grid operations.

ACKNOWLEDGMENTS

The authors would like to express their sincere gratitude to all individuals and institutions who contributed to the successful completion of this review. Their guidance, feedback, and support greatly assisted in enhancing the quality and depth of the research.

FUNDING INFORMATION

No funding was received or allocated for this work. The research was carried out without any financial support from external funding agencies, institutions, or organizations.

AUTHOR CONTRIBUTIONS STATEMENT

This journal uses the Contributor Roles Taxonomy (CRediT) to recognize individual author contributions, reduce authorship disputes, and facilitate collaboration.

Name of Author	C	M	So	Va	Fo	I	R	D	O	E	Vi	Su	P	Fu
Mitali Samal	✓	✓	✓	✓	✓	✓		✓	✓	✓			✓	
Chinmoy Kumar Panigrahi		✓				✓		✓	✓	✓	✓	✓		
Deepak Kumar Gupta	✓		✓	✓			✓			✓	✓		✓	✓

C : **C**onceptualization
M : **M**ethodology
So : **So**ftware
Va : **Va**lidation
Fo : **Fo**rmal analysis
I : **I**nvestigation
R : **R**esources
D : **D**ata Curation
O : Writing -**O**riginal Draft
E : Writing - Review &**E**diting
Vi : **Vi**sualization
Su : **Su**pervision
P : **P**roject administration
Fu : **Fu**nding acquisition

CONFLICT OF INTEREST STATEMENT

Authors state no conflict of interest.

DATA AVAILABILITY

The data used in this study are available from the corresponding author upon reasonable request. The simulation models, parameters, and results presented in this work were generated by the authors for the purpose of this research.

REFERENCES

[1] P. Kundur, *Power System Stability and Control*. McGraw- Hill, 1994.
[2] K. R. Padiyar, *Power System Dynamics: Stability & Control*, 2nd Editio. BS Publications/BSP Books, 2008.
[3] A. S. Debs, *Modern Power Systems Control and Operation*. Boston, MA: Springer US, 1988. doi: 10.1007/978-1-4613-1073-0.
[4] N. Paliwal, L. Srivastava, and M. Pandit, “PSO-based PID controller designing for LFC of single area electrical power network,” in *Nature Inspired Optimization for Electrical Power System*, 2020, pp. 43–54. doi: 10.1007/978-981-15-4004-2_4.

[5] M. K. Debnath, R. Agrawal, S. R. Tripathy, and S. Choudhury, "Artificial neural network tuned PID controller for LFC investigation including distributed generation," *International Journal of Numerical Modelling: Electronic Networks, Devices and Fields*, vol. 33, no. 5, Sep. 2020, doi: 10.1002/jnm.2740.

[6] M. Shouran and A. M. Alsseid, "Cascade of fractional order PID based PSO algorithm for LFC in two-area power system," in *2021 3rd International Conference on Electronics Representation and Algorithm (ICERA)*, IEEE, Jul. 2021, pp. 1–6. doi: 10.1109/ICERA53111.2021.9538646.

[7] M. Ahmed, M. Khamies, G. Magdy, and S. Kamel, "Designing optimal PI λ D μ controller for LFC of two-area power systems using African vulture's optimization algorithm," in *2021 22nd International Middle East Power Systems Conference (MEPCON)*, IEEE, Dec. 2021, pp. 430–437. doi: 10.1109/MEPCON50283.2021.9686297.

[8] N. Vafamand, M. M. Arefi, M. H. Asemani, and T. Dragicevic, "Decentralized robust disturbance-observer based LFC of interconnected systems," *IEEE Transactions on Industrial Electronics*, vol. 69, no. 5, pp. 4814–4823, May 2022, doi: 10.1109/TIE.2021.3078352.

[9] M. Ahmed, G. Magdy, M. Khamies, and S. Kamel, "Modified TID controller for load frequency control of a two-area interconnected diverse-unit power system," *International Journal of Electrical Power & Energy Systems*, vol. 135, p. 107528, Feb. 2022, doi: 10.1016/j.ijepes.2021.107528.

[10] M. Mokhtar, M. I. Marei, M. A. Sameh, and M. A. Attia, "An adaptive load frequency control for power systems with renewable energy sources," *Energies*, vol. 15, no. 2, p. 573, Jan. 2022, doi: 10.3390/en15020573.

[11] N. Kumar and A. Singh, "Load frequency control for multiarea power system using secondary controllers," *Trends in Sciences*, vol. 19, no. 2, p. 2044, Jan. 2022, doi: 10.48048/tis.2022.2044.

[12] A. H. A. Elkasem, M. Khamies, M. H. Hassan, A. M. Agwa, and S. Kamel, "Optimal design of TD-TI controller for LFC considering renewables penetration by an improved chaos game optimizer," *Fractal and Fractional*, vol. 6, no. 4, p. 220, Apr. 2022, doi: 10.3390/fractalfract6040220.

[13] S. Tripathi, V. P. Singh, N. Kishor, and A. S. Pandey, "Load frequency control of power system considering electric Vehicles' aggregator with communication delay," *International Journal of Electrical Power & Energy Systems*, vol. 145, p. 108697, Feb. 2023, doi: 10.1016/j.ijepes.2022.108697.

[14] J. Biswas, P. Bera, and K. Chakrabarty, "Determination of control area and design of fuzzy rule-tuned PID controller for LFC of multimachine power system," *Electric Power Systems Research*, vol. 221, p. 109411, Aug. 2023, doi: 10.1016/j.epsr.2023.109411.

[15] A. Oshnoei *et al.*, "Intelligent coordination of traditional power plants and inverters air conditioners controlled with feedback-corrected MPC in LFC," *IEEE Transactions on Circuits and Systems I: Regular Papers*, vol. 71, no. 1, pp. 473–484, Jan. 2024, doi: 10.1109/TCSI.2023.3330323.

[16] D. K. Gupta *et al.*, "Fractional order PID controller for load frequency control in a deregulated hybrid power system using Aquila Optimization," *Results in Engineering*, vol. 23, p. 102442, Sep. 2024, doi: 10.1016/j.rineng.2024.102442.

[17] P. Sharma and S. Neeli, "Computation of stability boundary locus of robust PID controller for time delayed LFC system," *International Journal of Dynamics and Control*, vol. 12, no. 5, pp. 1455–1465, May 2024, doi: 10.1007/s40435-023-01276-5.

[18] G. Dei *et al.*, "Improved squirrel search algorithm driven cascaded 2DOF-PID-FOI controller for load frequency control of renewable energy based hybrid power system," *IEEE Access*, vol. 10, pp. 46372–46391, 2022, doi: 10.1109/ACCESS.2022.3169749.

[19] S. K. Ojha and C. O. Maddela, "Load frequency control of a two-area power system with renewable energy sources using brown bear optimization technique," *Electrical Engineering*, vol. 106, no. 3, pp. 3589–3613, Jun. 2024, doi: 10.1007/s00202-023-02143-4.

[20] M. S. Iqbal, M. F. A. Limon, M. M. Kabir, M. K. M. Rabby, M. J. A. Soeb, and M. F. Jubayer, "A hybrid optimization algorithm for improving load frequency control in interconnected power systems," *Expert Systems with Applications*, vol. 249, p. 123702, Sep. 2024, doi: 10.1016/j.eswa.2024.123702.

[21] A. Sharma and N. Singh, "Load frequency control of connected multi-area multi-source power systems using energy storage and lyrebird optimization algorithm tuned PID controller," *Journal of Energy Storage*, vol. 100, p. 113609, Oct. 2024, doi: 10.1016/j.est.2024.113609.

[22] A. Awasthi, P. Khare, S. Yadav, A. Singh, and S. Goyal, "PSO based PID control approach for interconnected load frequency control scheme," in *2024 4th International Conference on Advance Computing and Innovative Technologies in Engineering (ICACITE)*, IEEE, May 2024, pp. 1772–1777. doi: 10.1109/ICACITE60783.2024.10616644.

[23] W.-M. Wang, H.-B. Zeng, J.-M. Liang, and S.-P. Xiao, "Sampled-data-based load frequency control for power systems considering time delays," *Journal of the Franklin Institute*, vol. 362, no. 2, p. 107477, Jan. 2025, doi: 10.1016/j.jfranklin.2024.107477.

[24] J. Hussain, R. Zou, S. Akhtar, and K. A. Abouda, "Design of cascade P-P-FOPID controller based on marine predators algorithm for load frequency control of electric power systems," *Electrical Engineering*, vol. 107, no. 1, pp. 809–827, Jan. 2025, doi: 10.1007/s00202-024-02551-0.

[25] M. F. A. Limon *et al.*, "Grey wolf optimization-based fuzzy-PID controller for load frequency control in multi-area power systems," *Journal of Automation and Intelligence*, vol. 4, no. 2, pp. 145–159, Jun. 2025, doi: 10.1016/j.jai.2025.01.002.

[26] P. Wang, J. Guo, F. Cheng, Y. Gu, F. Yuan, and F. Zhang, "A MPC-based load frequency control considering wind power intelligent forecasting," *Renewable Energy*, vol. 244, p. 122636, May 2025, doi: 10.1016/j.renene.2025.122636.

[27] S. C. Swain, B. K. Mahala, P. C. Sahu, S. K. Bhatta, G. G. Tejani, and S. J. Mousavirad, "Design and assessment of fuzzy controllers for LFC of multisource electrical system: A novel Sinh-Cosh (ShCh) technique," *Results in Engineering*, vol. 27, p. 106968, Sep. 2025, doi: 10.1016/j.rineng.2025.106968.

[28] N. EL Yakine Kouba, M. Menaa, M. Hasni, and M. Boudour, "A new optimal load frequency control based on hybrid genetic algorithm and particle swarm optimization," *International Journal on Electrical Engineering and Informatics*, vol. 9, no. 3, pp. 418–440, Sep. 2017, doi: 10.15676/ijeei.2017.9.3.1.

[29] M. Gheisarnejad, "An effective hybrid harmony search and cuckoo optimization algorithm based fuzzy PID controller for load frequency control," *Applied Soft Computing*, vol. 65, pp. 121–138, Apr. 2018, doi: 10.1016/j.asoc.2018.01.007.

[30] G. Chen, Z. Li, Z. Zhang, and S. Li, "An improved ACO algorithm optimized fuzzy PID controller for load frequency control in multi area interconnected power systems," *IEEE Access*, vol. 8, pp. 6429–6447, 2020, doi: 10.1109/ACCESS.2019.2960380.

[31] N. Sundararaju, A. Vinayagam, V. Veerasamy, and G. Subramaniam, "A chaotic search-based hybrid optimization technique for automatic load frequency control of a renewable energy integrated power system," *Sustainability*, vol. 14, no. 9, p. 5668, May 2022, doi: 10.3390/su14095668.

[32] N. Paliwal, L. Srivastava, and M. Pandit, "Application of grey wolf optimization algorithm for load frequency control in multi-source single area power system," *Evolutionary Intelligence*, vol. 15, no. 1, pp. 563–584, Mar. 2022, doi: 10.1007/s12065-020-00530-5.

[33] B. Abdollahzadeh *et al.*, "Puma optimizer (PO): a novel metaheuristic optimization algorithm and its application in machine learning," *Cluster Computing*, vol. 27, no. 4, pp. 5235–5283, Jul. 2024, doi: 10.1007/s10586-023-04221-5.

[34] S. K. Bhatta, S. Mohapatra, P. C. Sahu, S. C. Swain, and S. Panda, “Load frequency control of a diverse energy source integrated hybrid power system with a novel hybridized harmony search-random search algorithm designed Fuzzy-3D controller,” *Energy Sources, Part A: Recovery, Utilization, and Environmental Effects*, vol. 47, no. 1, pp. 10839–10862, Jun. 2025, doi: 10.1080/15567036.2021.1970860.

[35] A. Kumar, S. Chanana, and A. Kumar, “Analysis of new optimization technique MGO tuned FOIPDF controller in load frequency control,” *Electrical Engineering*, vol. 107, no. 7, pp. 8721–8742, Jul. 2025, doi: 10.1007/s00202-024-02441-5.

[36] M. S. Alam *et al.*, “High-level renewable energy integrated system frequency control with SMES-based optimized fractional order controller,” *Electronics*, vol. 10, no. 4, p. 511, Feb. 2021, doi: 10.3390/electronics10040511.

[37] R. Asghar, F. Riganti Fulginei, H. Wadood, and S. Saeed, “A review of load frequency control schemes deployed for wind-integrated power systems,” *Sustainability*, vol. 15, no. 10, p. 8380, May 2023, doi: 10.3390/su15108380.

[38] U. Raj and R. Shankar, “Optimally enhanced fractional-order cascaded integral derivative tilt controller for improved load frequency control incorporating renewable energy sources and electric vehicle,” *Soft Computing*, vol. 27, no. 20, pp. 15247–15267, Oct. 2023, doi: 10.1007/s00500-023-07933-3.

[39] A. Daraz *et al.*, “Frequency stabilization of interconnected diverse power systems with integration of renewable energies and energy storage systems,” *Scientific Reports*, vol. 14, no. 1, p. 25655, Oct. 2024, doi: 10.1038/s41598-024-76980-z.

[40] S. R. Nandanwar, N. P. Patidar, S. Panda, J. Thakkar, and M. L. Kolhe, “Synergistic control for enhancing frequency stability in grid-integrated network with decentralized renewable energy resources, energy storage, and electric vehicles,” *Cleaner Engineering and Technology*, vol. 20, p. 100757, Jun. 2024, doi: 10.1016/j.clet.2024.100757.

[41] M. A. Hossain, E. M. Gray, J. Lu, M. S. Alam, W. Hassan, and M. Negnevitsky, “Optimized model-free frequency control for renewable energy integration in islanded power systems,” *IEEE Transactions on Industry Applications*, vol. 62, no. 2, pp. 2084–2096, Mar. 2026, doi: 10.1109/TIA.2025.3603757.

[42] E. Şahin and M. S. Ayas, “Performance enhancement of PI and PIDn controllers through deep reinforcement learning for frequency regulation in renewable-integrated power systems,” *International Journal of Systems Science*, vol. 57, no. 5, pp. 1221–1238, Apr. 2026, doi: 10.1080/00207721.2025.2529476.

[43] M. A. El-Hameed, M. Saeed, A. Kabbani, and E. Abd El-Hay, “Efficient load frequency controller for a power system comprising renewable resources based on deep reinforcement learning,” *Scientific Reports*, vol. 15, no. 1, p. 18379, May 2025, doi: 10.1038/s41598-025-03310-2.

[44] I. Khan, S. A. Malik, A. Daraz, and B. Bareer, “Enhanced load frequency regulation in microgrids with renewable energy sources and electric vehicles,” *Scientific Reports*, vol. 15, no. 1, p. 26634, Jul. 2025, doi: 10.1038/s41598-025-10835-z.

[45] M. M. Ali *et al.*, “Enhancing power grid frequency stability with an optimized TID-MRAC controller and electric vehicle integration under renewable energy penetration,” *Neural Computing and Applications*, vol. 37, no. 23, pp. 19037–19061, Aug. 2025, doi: 10.1007/s00521-025-11298-z.

BIOGRAPHIES OF AUTHORS

Mitali Samal received the B.Tech. degree in electrical and electronics engineering in 2018 and the M.Tech. degree in electrical engineering in 2020 from IGIT Sarang, India. She is currently working as a teaching professional and pursuing a Ph.D. in the School of Electrical Engineering at KIIT Deemed to be University, Bhubaneswar, India. Her research interests include load frequency control in power systems, optimization techniques, renewable energy, and electric vehicles. She can be contacted at email: mitalisamal96@gmail.com.

Chinmoy Kumar Panigrahi is a distinguished academic and researcher, currently serving as a professor and Director of the School of Electrical Engineering at KIIT Deemed to be University, Bhubaneswar, India. He received his B.Sc. (Engg.) degree in electrical engineering from Sambalpur University in 1990, his M.E. degree from VSSUT University in 1998, and his Ph.D. (Engg.) degree from Jadavpur University in 2007. With over three decades of academic and research experience, he has supervised 33 Ph.D. scholars and made significant contributions to research in areas including soft computing, power electronics, electric vehicles, smart grids, battery management systems, power system applications, and renewable energy. He is actively involved in professional organizations, including IEEE and the Institution of Engineers (India). He has served as Vice Chair of the IEEE Bhubaneswar Section and currently serves as Chair of the IEEE Bhubaneswar Section PES Chapter. He is a Senior Member of IEEE. He can be contacted at email: panigrahichinmoy@gmail.com.

Deepak Kumar Gupta received his B.Tech. degree in electrical engineering from BBDNITM, Lucknow, in 2011 and his M.Tech. degree in power systems from NIT Hamirpur, Himachal Pradesh, in 2013. He completed his Ph.D. from IIT (BHU), Varanasi, in 2018. He served as an assistant professor in the School of Electrical Engineering at KIIT University, Bhubaneswar, Odisha, from 2017 to 2025. He is currently working as an assistant professor in the Department of Electrical Engineering at Netaji Subhas University of Technology (NSUT), New Delhi, India. His research interests include power system control, FACTS devices, optimization techniques, artificial intelligence, and renewable energy. He can be contacted at email: deepak.gupta@nsut.ac.in.